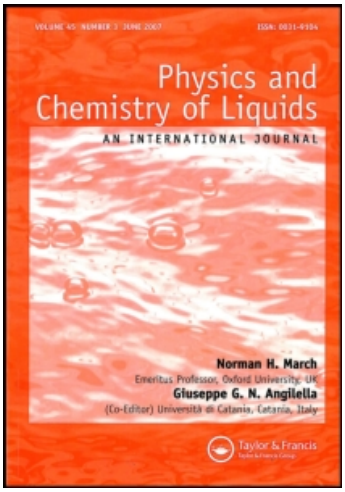

Physics and Chemistry of Liquids

Publication details, including instructions for authors and subscription information:
http://www.informaworld.com/smpp/title~content=t713646857

Interatomic Pair Potentials for Metallic Alloy Glasses

Ji-Chen Li[ab]; N. Cowlam[a]
[a] Department of Physics, University of Sheffield, Sheffield, UK [b] Department of Physics, Shandoug University, Jinan, Shandoug, Peoples Republic of China

To cite this Article Li, Ji-Chen and Cowlam, N.(1987) 'Interatomic Pair Potentials for Metallic Alloy Glasses', Physics and Chemistry of Liquids, 17: 1, 29 — 44
To link to this Article: DOI: 10.1080/00319108708078539
URL: http://dx.doi.org/10.1080/00319108708078539

Phys. Chem. Liq., 1987, Vol. 17, pp. 29–44
Photocopying permitted by license only

Printed in the United Kingdom

Interatomic Pair Potentials for Metallic Alloy Glasses

JI-CHEN LI* and N. COWLAM

Department of Physics, University of Sheffield, Sheffield S3 7RH, UK

(Received 24 November 1986)

The derivation of interatomic potentials for metallic alloy glasses is discussed. First, a comparison is made between the derivation of the radial distribution function RDF (and its associated curves) and that of the interatomic pair potential $\phi(r)$, starting from the same structure factor $S(Q)$. This comparison illustrates how different components of the $S(Q)$ curve influence the course of the two derivations. A determination of the three interatomic pair potentials $\phi_{NiNi}(r)$, $\phi_{NiP}(r)$, $\phi_{PP}(r)$ for a $Ni_{80}P_{20}$ metallic glass is then given to illustrate the method. The use of such potentials in structural relaxation calculations is then discussed for both single component and binary cases. Comparison is made between calculated and experimental structure factor $S(Q)$ curves with very encouraging results. Finally, the possible future extension of these calculations is examined.

Key words: Interatomic potentials, radial distribution function, $Ni_{80}P_{20}$ metallic glass, structure factor.

1 INTRODUCTION

We have discussed in a recent paper in this journal[1] the possibility of deriving the interatomic pair potentials from diffraction data on metallic alloy glasses, by using those methods applied originally to the study of simple liquid metals[2]. These involve deriving the direct correlation function $c(r)$ from the structure factor $S(Q)$ and the pair potential $\phi(r)$ from $c(r)$ by using one of the established identities[2].

The motivation for this was to explore the general applicability of the method and to find whether the pair potentials obtained exhibited any particular features which might influence their use in relaxation and molecular dynamics calculations, rather than to try to suggest that

* Permanent address: Department of Physics, Shandoug University, Jinan, Shandoug, Peoples Republic of China.

simple theory could be applied to such relatively complex systems as binary metallic glasses.

Encouraging results were obtained in the preliminary work[1]. Specifically, the derivation of the pair potential $\phi(r)$ for a pseudo single-component system was found to lead, fairly straightforwardly, to curves with a minimum at the expected interatomic spacing and a well-depth of the correct magnitude[1]. Only the repulsive hard-core part of the potential was poorly represented because the identities used are strictly speaking asymptotic results which are not valid at small r values[2]. All the pair potential curves obtained exhibited positive and negative oscillations beyond the first minimum, which did not, however, follow the $\cos(2k_F r)/r^3$ dependence of the Freidel oscillations. The derivation of the three independent pair potentials $\phi_{11}(r)$, $\phi_{12}(r)$, $\phi_{22}(r)$ for a binary case turned out to be more difficult. As will be shown in Section 3, the intermediate functions $c_{11}(Q)$, $c_{12}(Q)$, $c_{22}(Q)$ required depend on small differences in the three *partial* structure factors[3] $S_{11}(Q)$, $S_{12}(Q)$, $S_{22}(Q)$ which themselves are derived from (small) differences between three different *total* structure factors $S(Q)$ measured experimentally. Thus the derivation of pair potentials, represents a second generation of analysis and makes extreme demands on the quality of the original experimental data.

We have continued work in this area and recently achieved a successful derivation of all three pair potentials for a binary metallic glass $Ni_{80}P_{20}$[4] rather than for just the majority (Ni–Ni) component in the $Ni_{64}B_{36}$ glass of our original investigation[1]. In this present paper the derivations of both $\phi(r)$ and radial distribution factor (RDF) curves are first compared and then details of the new derivation for $Ni_{80}P_{20}$ presented. The pair potentials obtained in this work are then used in relaxation calculations to show that they lead to reasonable real-space structures and comparison is also made with relaxed structures derived using Lennard-Jones 6–12 potentials. Details of this work have already been presented in abstract form[5,6].

2 STRUCTURAL MEASUREMENTS AND INTERATOMIC POTENTIALS FOR LIQUIDS AND GLASSES

It was concluded in our previous investigation[1] that only the very best diffraction data currently available would permit an unambiguous determination of the three pair potentials for a binary glass to be made, in view of the extreme demands on the quality and consistency of the data in the analysis. It was crucial therefore, in the search for candidates to continue this work, to be able to identify those features of $S(Q)$ curves

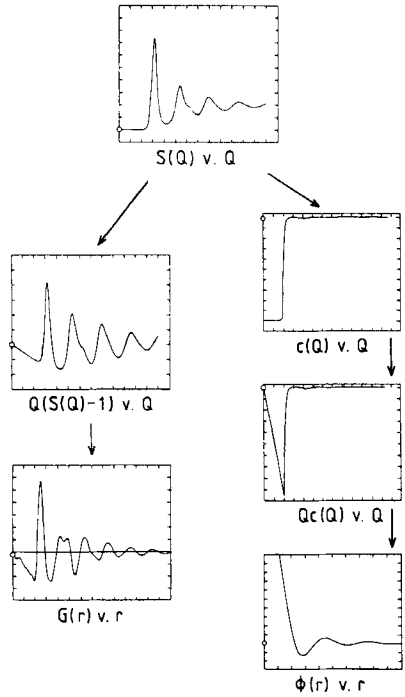

Figure 1 The derivations of the reduced RDF $G(r)$ and the interatomic pair potential $\phi(r)$, starting from the same structure factor $S(Q)$ of a one-component liquid or glass, are shown schematically. The graphs on the left hand side show the normal route for structure determination, the product $Q(S(Q) - 1)$ which is Fourier transformed to give the reduced RDF $G(r)$. On the right hand side the alternate derivation of $\phi(r)$ is shown with graphs of $c(Q) = 1 - 1/S(Q)$, $Qc(Q)$, and $\phi(r) = -kTc(r)$. The origin of each graph is shown by an open circle.

which are most significant in determining a reliable $\phi(r)$ function and also to monitor the effect of various uncertainties in $S(Q)$ on the form of the $\phi(r)$ which is obtained.

Figure 1 shows schematically the two routes by which an experimentally-obtained structure factor curve $S(Q)$ may be analysed. (A single component system is considerd here for convenience and it is supposed that all the corrections and the normalisation necessary to obtain $S(Q)$ from the measured intensity distribution $I(Q)$ have been successfully completed.) On the left hand side of Figure 1 is the normal route for structural measurements. The quantity $Q(S(Q) - 1)$ appears in the sine Fourier Transform used to obtain the reduced radial distribution function $G(r)$ from which the RDF $4\pi r^2\rho(r)$ may also be obtained.

$$G(r) = 4\pi r(\rho(r) - \rho_0) = \frac{2}{\pi}\int_0^\infty Q(S(Q) - 1)\sin Qr\, dQ \qquad (1)$$

Although it is sometimes misleading to attempt to associate individual features of $S(Q)$ or $Q(S(Q) - 1)$ with particular features of $G(r)$ it is well established that the first peak of $Q(S(Q) - 1)$ is the most important part which largely determines the position of the first peak in $G(r)$ and the wavelength of the oscillations in $G(r)$ at larger radial distances. This correlation has been established in several ways; by the modified Bragg equations sometimes adopted for amorphous materials—as discussed by Klug and Alexander[7]; by the more direct analysis of the sine Fourier transform itself[8] and by a practical example in which the whole of the $S(Q)$ was substituted by a single Gaussian centred at the first peak—see Cargill[9], his Figure 12. This latter result has also been confirmed in the course of the present calculations by subdividing $S(Q)$ and making transforms of various portions of the complete curve[10]. The product $Q(S(Q) - 1)$ appears in the transform, Eq. 1, so that the shape of $S(Q)$ in the *small* Q region and the way $S(Q)$ approaches the limit $S(0)$ has little influence on the form of $G(r)$ and this has also been demonstrated by practical examples[11].

The derivation of $\phi(r)$ from $S(Q)$ is shown in the right-hand side of Figure 1. The $c(Q)$ curve[1],

$$c(Q) = 1 - \frac{1}{S(Q)} \tag{2}$$

is dominated by large negative values, of the order of a few hundreds, at small Q whose magnitudes are determined by the compressibility limit $S(0)$, see Ref. 2 for example, while the steep rise of $c(Q)$ up to the abscissa in influenced by the $S(Q)$ values at the foot of the first peak. The first peak in $S(Q)$ gives an insignificantly small positive first peak in $c(Q) \approx 0.7$. The direct correlation function $c(r)$ is derived from the sine Fourier transform of $Qc(Q)$

$$c(r) = \frac{1}{2\pi^2 \rho_0 r} \int_0^\infty Qc(Q) \sin Qr \, dQ \tag{3}$$

and from this the pair potential $\phi(r)$ can be obtained using the relation[12],

$$\phi(r) = -kTc(r) \tag{4}$$

It is tempting, in view of the negative sign in Eq. (4), to associate the steep rise in $c(Q)$ with the repulsive core part of $\phi(r)$. However, it is the product $Qc(Q)$ which is quite different from $c(Q)$, which is transformed. The product $Qc(Q)$ effectively removes the value of the compressibility limit at $Q = 0$ (except as it influences the slope of $Qc(Q)$ for small Q values) while the area under the $Qc(Q)$ curve determines the $\phi(0)$ value.

In an extreme case as shown in Figure 1, the dominant, first negative peak of $Qc(Q)$ effectively determines $\phi(r)$ completely, so that there is no practical difference between the transform of the whole curve and the curve truncated at the first point it crosses the abscissa. In this case, the first maximum in $S(Q)$—which is so important in the transform to $G(r)$, has virtually no influence in determining the form of $\phi(r)$. However, in real examples of binary alloys, the first negative peak in the equivalent $Qc_{ij}(Q)$ curve may be very much less well developed, so that the first positive peak can also influence the precise position of the minimum of the potential well. Again this has been demonstrated by transforming various portions of a complete $Qc_{ij}(Q)$ curve[10].

3 THE DERIVATION OF PAIR POTENTIALS FOR $Ni_{80}P_{20}$ METALLIC GLASS

As discussed more fully in the previous work[1], the Eqs 2, 3 and 4 above may be generalised for binary alloys and an identification made

$$\phi_{ij}(r) = -kTc_{ij}(r) \quad \text{where } i = 1, 2 \tag{5}$$

The chief difference in the binary case is that the functions $c_{ij}(Q)$ are now expressed in terms of differences between all three partial structure factors $S_{ij}(Q)$, so that

$$\begin{aligned} c_{11} &= [(S_{11} - 1)(1 + x_2(S_{22} - 1)) - x_2(S_{12} - 1)^2]/D \\ c_{12} &= (S_{12} - 1)/D \\ c_{22} &= [(S_{22} - 1)(1 + x_1(S_{11} - 1)) - x_1(S_{12} - 1)^2]/D \end{aligned} \tag{6}$$

where

$$D = [1 + x_1(S_{11} - 1)][1 + x_2(S_{22} - 1)] - x_1x_2(S_{12} - 1)^2 \tag{7}$$

and the Q dependence of $c_{ij}(Q)$ and $S_{ij}(Q)$ has been omitted for brevity. This makes the accurate determination of the $c_{ij}(Q)$ much more difficult. For example, only the pair potential $\phi_{NiNi}(r)$ of the majority constituent in a $Ni_{64}B_{36}$ glass could be derived with any precision in our previous work[1].

However, there have been a number of recent determinations of partial structure factors of binary metallic glasses chiefly involving neutron experiments on isotope enriched samples[13–18]. In those cases, the quality of the results is enhanced by both the favourable conditioning of the three simultaneous equations needed to derive the partial $S(Q)$'s (in comparison with earlier X-ray work) and the high statistical

quality of data from the current neutron diffractometers. We have examined the results of these recent determinations of partial structure factors[13–18] with a view to obtaining *all three* pair potentials by the route outline in Eqs 5, 6 and 7 above. The partial $S(Q)$ curves for $Ni_{81}B_{19}$ glass[13] provided the first evidence that the method might be successful[5] but required some small modification at small Q values. However, the partial $S(Q)$ curves for $Ni_{80}P_{20}$ glass from the same laboratory[4], have demonstrated unequivocally that the derivation can be made without any adjustment. It was only necessary to extrapolate the three curves $S_{NiNi}(Q)$, $S_{NiP}(Q)$, $S_{PP}(Q)$ down to $Q = 0$ by lines which were drawn freehand and the $c_{ij}(Q)$ functions were obtained directly from the $S_{ij}(Q)$ using Eqs 6 and 7. The Fourier transforms of the $c_{ij}(Q)$ were made and the pair potentials $\phi_{ij}(r)$ obtained from Eq. 5 using a characteristic temperature of 300 K as before[1]. The resulting $\phi_{ij}(r)$ are shown in the upper part of Figure 2 with Lennard-Jones 6–12 potentials superimposed, to provide the repulsive hard core. Once again it is found that all three pair potentials have their first minimum at values within 5% expected distances, based on the Goldschmidt diameter of nickel

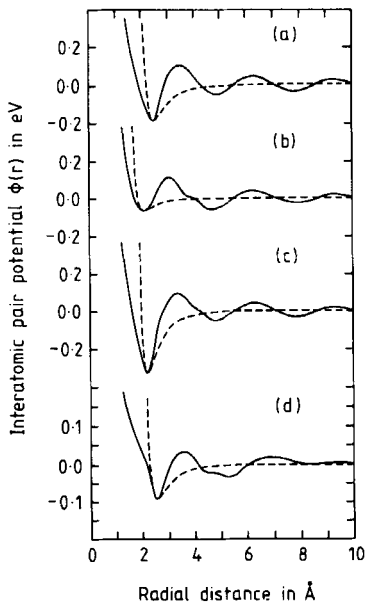

Figure 2 The three pair potentials (a) $\phi_{NiNi}(r)$, (b) $\phi_{PP}(r)$, (c) $\phi_{NiP}(r)$ for $Ni_{80}P_{20}$ metallic glass obtained directly from the experimental partial structure factors[4] are shown. Lennard-Jones potentials are superimposed (dotted lines) to provide the repulsive core of the potential. Figure 2a shows the $\phi_{NiNi}(r)$ potential derived from experimental data on $Ni_{63.7}Zr_{36.3}$ glass[16]. Parameters for these derived potentials are given in Table 1.

Table 1 Parameters for the pair potentials shown in Figure 2 are given. ε_0 and r_0 are the depth and position of the potential minimum, r'_0 the second minimum. r_1 and r_2 are the radial distances to the positive maxima.

Pair potential	Potential well				Positive oscillations			
	ε_0 (eV)	r_0 (Å)	r'_0 (Å)	$\langle r_0 \rangle$ (Å)	r_1 (Å)	r_2 (Å)	r_1/r_0	r_2/r_0
$\phi_{NiNi}(r)$	−0.19	2.53	—	2.48	3.56	6.29	1.41	2.49
$\phi_{NiP}(r)$	−0.32	2.24	—	2.34	3.38	6.39	1.51	2.85
$\phi_{PP}(r)$	−0.06	2.10	4.72	2.20	3.11	6.24	1.49	2.98
$\phi_{NiNi}(r)$	−0.10	2.56	—	2.48	3.61	6.90	1.37	2.69

2.48 Å and the tetrahedral covalent radius of phosphorus 1.1 Å—see Table 1. The well depths ε_0 for each potential are of the order of ~0.1 eV (Table 1) and are commensurate with values obtained previously and those quoted in the literature[1]. It is interesting that $\phi_{NiP}(r)$ shows the deepest potential well of the three curves which is presumably an indication of strong chemical interactions between the two species. In addition whilst all three potential curves show quite strong oscillations beyond the first minimum, in the case of $\phi_{PP}(r)$ this results in two successive minima of almost equal depth. This may have interesting implications for the structures of $TM_{80}met_{20}$ type glasses as discussed more fully in Section 5.

The fourth curve in Figure 2 is the $\phi_{NiNi}(r)$ pair potential derived by us from structural data on a $Ni_{63.7}Zr_{36.3}$ glass[16] using the same methods. This was chosen as a fairly representative example of a majority $\phi_{TMTM}(r)$ pair potential (in showing well-developed oscillations at large r values) for the trial relaxation calculations on a single component array to be described in Section 4.1. This potential is also shown with a 6–12 potential which provided the repulsive core. The oscillations in the pair potentials shown in Figure 2 appear to be more regularly developed than in the cases derived by us previously[1]. However, a $\cos(2k_F r)/r^3$ dependence leads to a value $k_F \sim 0.8\,\text{Å}^{-1}$ whilst the identification $Q_1 = 2k_F$ for the first maximum in $S(Q)$ gives $k_F \sim 1.5\,\text{Å}^{-1}$—except for the first broad peak in $S_{PP}(Q)$. This disagreement in the k_F values was also observed in the earlier work[1].

4 RELAXATION CALCULATIONS ON DISORDERED ATOMIC ARRAYS

It has been shown in the previous work[1] and in Section 3 above that pair potentials with the normally accepted characteristics can indeed be obtained from diffraction data for metallic alloy glasses. However, it is

important to try to assess the authenticity of these pair potentials and one way of doing this is by using them in structural relaxation calculations on model metallic glass arrays. In this section two such examples are presented—a trial case on a small single-component cluster and a second calculation on a larger binary array. Structural relaxation calculations are important not only in giving realistic densities to hand-built and computer models of metallic glass structures, but also because of their relation to the low temperature heat treatments which are used to improve the magnetic properties of ferromagnetic metallic glasses. These heat treatments result in a loss of free volume.

Structural relaxation calculations can be described as follows[19]. The total force on an atom n at $\underline{r}_n$ in a glassy structure is given by the sum of pair forces between atoms

$$\underline{F}_n(\underline{r}_n) = \sum_{m \neq n} \underline{F}_{nm}(r_{nm}) \tag{8}$$

If the atom n is displaced a distance $\delta\underline{r}_n$ while all the other atoms are kept fixed, then the change in the force is given by[19],

$$\underline{F}_n(r_n + \delta r_n) = \underline{F}_n(r_n) + (\delta\underline{r}_n \cdot \nabla)\underline{F}_{nm}(\underline{r}_{nm}) \tag{9}$$

The force-free position of atom n is then,

$$\underline{F}_n(r_n + \delta\underline{r}_n) = 0 \tag{10}$$

or

$$-\underline{F}_n(\underline{r}_n) = (\delta\underline{r}_n \cdot \nabla)\underline{F}_{nm}(\underline{r}_{nm}) \tag{11}$$

so that the displacements $\delta\underline{r}_n$ can be determined from Eq. 11 and the $\delta\underline{r}_n$ for all atoms calculated in turn. This procedure can be done iteratively by computer. Usually fractions of $\delta\underline{r}_n$ are added to a given atom in turn, to bring the force to zero, before proceeding to the next atom. Alternatively, as in the present program, the size of the step can be chosen automatically in relation to the magnitude of the force. Nine values of step between 0.03 Å and 0.0001 Å were available in the calculation. Surface effects can be very important in such calculations on finite arrays because the surface atoms experience less total force and this can lead to density gradients. In the present calculations these have been circumvented by means of a surface tension-type force. The magnitude of this force depended on the number of (absent) neighbours and the distance of the nth atom from its reduced complement of neighbours, while the direction was determined by the vector sum of the forces due to the neighbours present. The configurational energy was

monitored to test the effectiveness of the relaxation as the calculation proceeded. In this relatively simple kind of relaxation the effect of densification on the form of the force and potential curves is not taken into account, see Ref. 20 for example.

4.1 Relaxation of a one-component glassy structure

Trial calculations were made, as with the previous work[1], on a one-component structure. The $\phi_{NiNi}(r)$ pair potential shown in the lower part of Figure 2 was used together with a 6–12 potential to provide the repulsive core. The unchanged 6–12 potential was also used in a parallel calculation to provide a comparison. Both potentials were tabulated as data for the program in the form of 5000 values of interatomic force separated by 0.002 Å for $0 < r < 10$ Å. The atomic coordinates used as the starting point of the calculation were derived from position measurements of 140 polystyrene spheres, contained in a shallow curved dish to avoid regular (i.e. crystalline) geometries. This array had been used in a separate investigation[21]. It is shown in its original form in the left hand side of Figure 3 together with the final, compact, spherical shape of the array after relaxation with the boundary forces applied. It took typically 20 iterative passes over the 140 atoms present, calculating interatomic forces out to a range of 9 Å, to produce a stable (change-free) structure. This took of the order of 25

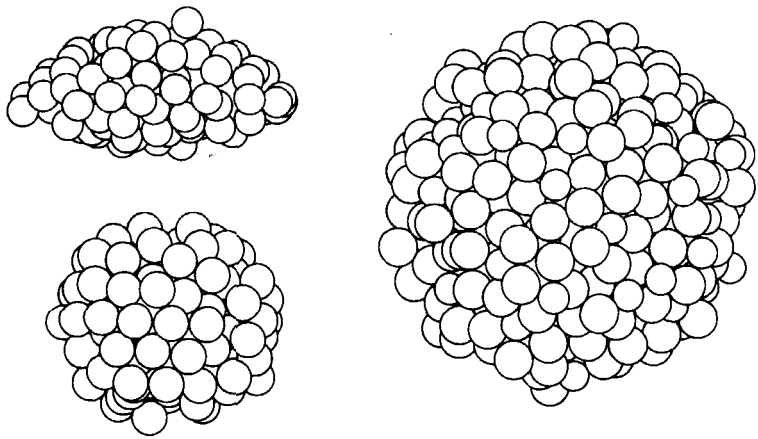

Figure 3 The 140 atom, single component array used in the trial relaxation calculation is shown in the left hand side of the Figure. The upper diagram shows the initial configuration and the lower diagram the final compact form after relaxation. In the right-hand side of the Figure the 530 atom binary array used in the relaxation calculation for $Ni_{80}P_{20}$ glass is shown in its relaxed state.

minutes CPU time on an IBM 3083 computer. The structures produced by this relaxation, using both the potentials, were rather similar and showed the characteristic features expected for metallic alloy glasses. The pair correlation function $g(r) = \rho(r)/\rho_0$ can be evaluated readily from the atomic coordinates and is shown in Figure 4. The structure factor $S(Q)$ can also be derived from $g(r)$ in the usual way and is also shown in Figure 4. The $\phi_{NiNi}(r)$ potential leads to a broader first peak in $g(r)$ than the 6–12 potential and the magnitudes of the second peak and its shoulder and of the subsequent oscillations in $g(r)$ were more reliably reproduced. In $S(Q)$, the $\phi_{NiNi}(r)$ potentials again led to a second peak shoulder of the accepted form—which was not so well reproduced with the 6–12. We have previously observed that these split second peaks in $g(r)$ and $S(Q)$ (which are characteristic of metallic glass structures) can be well reproduced in models built on surfaces having single or, as here, double curvature[21].

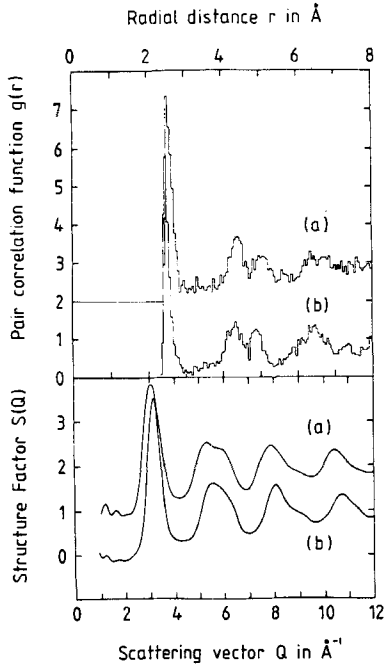

Figure 4 The pair correlation function $g(r) = \rho(r)/\rho_0$ derived from the coordinates of the 140 atom array after structural relaxation is shown together with the total structure factor $S(Q)$ derived from $g(r)$. The upper curve (a) corresponds in each case to the use of the composite $\phi_{NiNi}(r)$ potential of Figure 2 and the lower curve (b) to the use of a 6–12 potential.

Thus the conclusion of a trial calculation using a small array was that the derived $\phi_{NiNi}(r)$ performed at least as well as the 6–12 potential in a conventional relaxation calculation.

4.2 Relaxation of a $Ni_{80}P_{20}$ glassy structure

A second calculation was then performed to evaluate the three composite pair potentials made by combining the three curves $\phi_{NiNi}(r)$, $\phi_{NiP}(r)$, $\phi_{PP}(r)$ obtained from diffraction data on $Ni_{80}P_{20}$ glass in Section 3, with 6-12 potentials to provide a repulsive core as shown in Figure 2. The starting point in this case was an array of 530 equal sized polystyrene spheres constructed in the course of a separate investigation[21]. In order to portray this model (see Figure 3) 424 spheres were given a diameter of 2.48 Å (Ni) and 106 a diameter of 2.2 Å (P)—although in a relaxation calculation the atomic size does not have the same strict meaning as in a hard-sphere model. The computer program was developed from that used for the relaxation of the single component array, but with the force chosen according to the types of atoms (Ni or P) out to the same range of 9 Å. A consequence of these changes and the larger number of atoms present was that the new array needed up to 90 iterations before a stable state was obtained. This used up to 120 minutes CPU time. The 530 atom array is shown, after relaxation, in Figure 3.

The structures obtained in these relaxation calculations were evaluated by first obtaining the partial pair correlation functions $g_{ij}(r) = \rho_{ij}(r)/\rho_{0j}$ from the position coordinates of the appropriate atoms in the array. The central core of 380 atoms was used to avoid spurious effects due to the surface of the array. The partial structure factors $S_{ij}(Q)$ were then derived from the $g_{ij}(r)$ functions and compared directly with the experimental partial structure factors[4] which formed the starting point of this work, in Section 3. The comparison is shown in Figure 5. The calculated $S(Q)$'s have been derived from the array relaxed via the composite potentials of Figure 2 and with a *random distribution* of phosphorus atoms throughout. Although the experimental $S_{NiNi}(Q)$ and $S_{NiP}(Q)$ curves are reasonably well reproduced the agreement for $S_{PP}(Q)$ is poor over the whole curve. In order to try and improve the agreement modifications were made to the starting array, to move the metalloid atoms apart. This was done by building two constraints into the way in which the atoms were labelled within the array. First, if atom i and atom j were both phosphorus and $|\underline{r}_i - \underline{r}_j| < 2.2$ Å then atom j was replaced by nickel. Second, using each nickel atom as an origin in turn, the atoms within a sphere of radius 2.5 Å were examined and if no

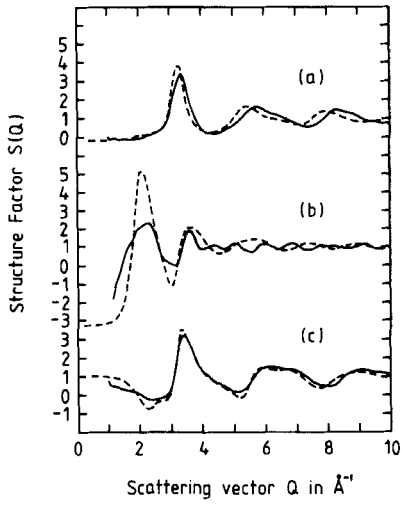

Figure 5 The partial structure factors (a) $S_{NiNi}(Q)$; (b) $S_{PP}(Q)$ and (c) $S_{NiP}(Q)$ derived from the 530 atom array (solid line) are compared with the experimental curves[4] (dotted line). The structural relaxation has been made with the composite potentials of Figure 2 and a random arrangement of phosphorus atoms in the binary array.

phosphorus atoms were found then the nickel atom at the origin was replaced by a phosphorus atom. In this way all first neighbour atom pairs were removed. Although a slight ($\sim 5\%$) excess concentration of phosphorus atoms developed at the surface after applying these constraints, the alloy composition within the central 380 atom core of the array remained unchanged.

Relaxation calculations were then repeated on the whole 530 atom array using composite and 6–12 potentials as before. The partial $S(Q)$ curves which resulted are shown in Figure 6. As before these are derived from the central 380 atoms of the array. There is a great improvement in the reproduction of the $S_{PP}(Q)$ curve in this case, in fact the overall agreement between experiment and calculation is surprisingly good. Even quite minor features in the $S(Q)$ curves such as those at the feet of the first peak in $S_{NiNi}(Q)$ and $S_{NiP}(Q)$ are reasonably well reproduced. The main disagreements are in the height of the first peak in $S_{PP}(Q)$ and in the same curve around 5.5 $Å^{-1}$.

Finally, although the 6–12 potentials give broadly similar results to the composite potentials, in detail the $S_{ij}(Q)$ curves obtained do not show the same measure of agreement with the experimental curves. The most serious fault is that the position of the first (and other) peaks in the major partial $S_{NiNi}(Q)$ are predicted to occur at higher Q values than are observed, see Table 2. The tabulated force curves were checked to

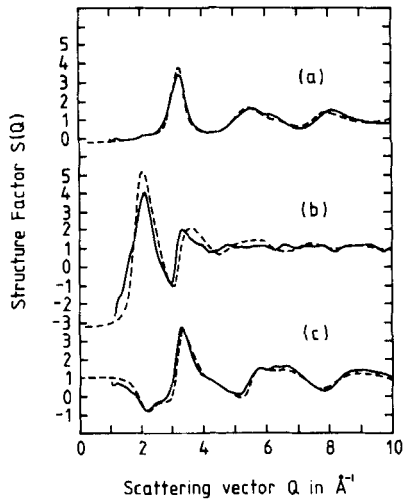

Figure 6 The partial structure factors (a) $S_{NiNi}(Q)$; (b) $S_{PP}(Q)$ and (c) $S_{NiP}(Q)$ derived from the 530 atom array (solid line) are compared with the experimental curves[4] (dotted line). The same potentials have been used as in Figure 5 but with the atoms of the array re-identified to avoid first neighbour phosphorus-phosphorous pairs.

Table 2 The partial coordination numbers obtained from the 580 atom binary array when structurally relaxed under different conditions, together with the peak positions of the partial structure factors derived from them, are compared with the experimental values[4].

Starting conditions of binary array	First peak position in partial $S_{ij}(Q)$			Partial coordination number from RDF's		
	$S_{NiNi}(Q)$	$S_{NiP}(Q)$	$S_{PP}(Q)$	n_{NiNi}	n_{NiP}	n_{PP}
Experiment[4]	3.26	3.33	2.09	9.4	2.3	5.3
Composite potentials random P atoms	3.24	3.33	2.23	9.2	2.6	6.7
Composite potentials no P-P first neighbours	3.27	3.34	2.10	9.3	2.6	5.3
6-12 potentials random P atoms	3.34	3.44	—	9.1	2.5	6.4
6-12 potentials, no P-P first neighbours	3.33	3.41	2.16	9.1	2.5	4.5

ensure that this could not be due to slightly different positions of zero force for the 6–12 and composite potentials. However, unlike the composite case, the 6–12 potential is attractive for *all distances* beyond the minimum. It is possible therefore that when the range over which the interatomic forces are calculated is substantial, that this might lead to an overdensification of the majority (nickel) component in the array, giving rise to slightly smaller values of interatomic distance and hence an expanded abscissa to the $S_{NiNi}(Q)$ curve. This effect would not arise to the same extent with an oscillatory force which changed sign several times over the range in which the interatomic forces were being computed.

5 CONCLUSIONS

These investigations have been undertaken to discover whether the methods for the determination of interatomic pair potentials of liquid metals might also work for metallic alloy glasses and to determine whether the potentials obtained might exhibit any distinctive features. Leaving aside the question of whether the theoretical results for a liquid metal in equilibrium (on which the method is based) can be applied equally well to a metastable metallic glass, together with the associated problem of the determination of the long wavelength limits of the structure factors, it appears nevertheless that useful results can be obtained in this area.

Furthermore there is an additional bonus, that independently of the form of the pair potentials obtained, their derivation provides a very valuable monitor of the correctness of experimental curves particularly at small Q values. This has emerged from our examination of a number of the recent experimental determinations of partial structure factors for metallic alloy glasses and this will be described in detail elsewhere[22].

With regard to the form of the pair potential curves obtained, the accumulated evidence suggests that the oscillations in $\phi(r)$ beyond the first minimum are real, while the relaxation calculations show that these oscillations are significant in determining the details of the glassy structure produced. This was shown by direct comparison of oscillatory and non-oscillatory (6–12) potentials for single component, random and non-random binary arrays. It will obviously be interesting to establish whether such oscillatory potentials can be used in a 'first principles' derivation of metallic glass structure, say by molecular dynamics calculations—rather than the relaxation calculations undertaken here.

The most extreme form of oscillatory potential is observed in $\phi_{PP}(r)$, see Figure 2, in which two successive minima of almost equal depth are observed. This is interesting on account of the debate over the possible presence, or absence, of first neighbour metalloid-metalloid atoms in Transition $metal_{80}metalloid_{20}$ type glasses such as $Ni_{80}P_{20}$. In the 1970's Polk[23] proposed an essentially interstitial model for $TM_{80}met_{20}$ glasses in which first neighbour metalloid pairs were rigidly excluded. We have argued recently[14,24] that small numbers of metalloid first neighbours may be more consistent with diffraction data than none. This is also supported by recent structural simulation[25,26] which indicates that the metalloid atoms are too large to be accommodated interstitially at least at the 20% concentration. A $\phi_{metmet}(r)$ potential with two minima is therefore interesting in that the first minimum might be associated with small numbers of met-met first neighbours (with a coordination number of say ≤ 0.5 atoms—much smaller than the 2.4 atoms expected in a random occupation of a 12 atom first neighbour shell). The second minimum could be associated with the more distant met-met pairs described in the original interstitial models of $TM_{80}met_{20}$ glasses[23]. At present, the success achieved in the relaxation calculation by the exclusion of first neighbour phosphorus atoms appears to contradict this kind of description of the potential with two minima but clearly such curves are worthy of further investigation.

In our previous work[1] the hope was expressed that the derivation of all three pair potentials for binary metallic glasses might allow accurate models of their structures to be simulated successfully without constraints being imposed. This has not happened for the relaxation calculations presented here, but this is likely to be a consequence of the relatively restricted atomic mobility in such structural rearrangements. An obvious next step is therefore to investigate the possibility that molecular dynamics simulations can overcome this restriction and create the appropriate structures for binary glasses outright and this is the subject of our current work.

Acknowledgements

This work has arisen from a programme supported in personnel and materials by the SERC. One of the authors (J-C Li) acknowledges the award of a Robert Styring Scholarship of the University of Sheffield. Both authors would like to thank Miss A. C. Strange and Mr. S. E. Hayward who, during undergraduate project work, began to show that the derivation of the three pair potentials for a binary glass was not quite such an impossible task as the previous attempt on $Ni_{64}B_{36}$ had suggested.

References

1. N. Cowlam, K. Dini, P. P. Gardner and H. A. Davies, *Phys. Chem. Liq.*, **15**, 253, 1986.
2. N. H. March, *Liquid Metals*, Pergamon Press, Oxford (1968).
3. T. E. Faber and J. M. Ziman, *Phil. Mag.*, **11**, 153, 1965.
4. P. Lamparter and S. Steeb, Proc. 5th Int. Conf. Rap. Quen. Met. (North Holland: Amsterdam), 1, 459, 1985.
5. N. Cowlam, K. Dini, P. P. Gardner, A. C. Strange, S. E. Hayward, J.-C. Li and H. A. Davies, Recent developments in non-crystalline metallic materials, Bad Honnef, 1986 (Abstract).
6. J.-C. Li and N. Cowlam, Rapid Solidification Conference, University of Surrey, 1986 (Abstract).
7. H. P. Klug and L. E. Alexander, *X-ray diffraction procedures*, J. Wiley, New York (1974).
8. C. Finbak, *Acta. Chem. Scand.*, **3**, 1279, 1949.
9. G. S. Cargill III, *Sol. Stat. Phys.*, **30**, 227, 1975.
10. J.-C. Li (unpublished material).
11. A. C. Wright (private communication).
12. M. I. Barker and T. Gaskell, *Phys. Lett.*, **53A**, 285, 1975.
13. P. Lamparter, W. Sperl, S. Steeb and J. Blétry, *Z. Natforschung*, **37a**, 1223, 1982.
14. N. Cowlam, Wu Guoan, P. P. Gardner and H. A. Davies, *J. Non. Cryst. Sol.*, **61 + 62**, 337, 1984.
15. T. Fukunaga, N. Watanabe and K. Suzuki, *J. Non. Cryst. Sol.*, **61 + 62**, 343, 1984.
16. S. Lefebvre, R. Bellissent, A. Quivy, J. Bigot and Y. Calveyrac, *J. Phys. F.: Met. Phys.*, **15**, L99, 1985.
17. T. Fukunaga, N. Hayashi, N. Watanabe and K. Suzuki, Proc. 5th Int. Conf. Rap. Quen. Met. (North Holland: Amsterdam), **1**, 475, 1985.
18. M. Maret, P. Chieux, P. Hicter, M. Atzmon and W. L. Johnson, Proc. 5th Int. Conf. Rap. Quen. Met. (North Holland: Amsterdam) **1**, 521, 1985.
19. L. von Heimendahl, *J. Phys. F.: Met. Phys.*, **9**, 161, 1979.
20. J. Hafner and G. Punz, *J. Phys. F.: Met. Phys.*, **13**, 1393, 1983.
21. J.-C. Li and N. Cowlam (to be published).
22. J.-C. Li, He Fenglai and N. Cowlam (to be published).
23. D. E. Polk, *Acta. Met.*, **20**, 485, 1972.
24. Wu Guoan, N. Cowlam, K. R. A. Ziebeck, H. A. Davies (to be published).
25. J. F. Finney and J. Wallace, *J. Non. Cryst. Sol.*, **43**, 165, 1981.
26. F. Lançon, L. Billard and A. Chamberod, *J., Phys. F.: Met. Phys.*, **14**, 579, 1984.